Journal of
www. biophotonics-journal.org
BIOPHOTONICS

FULL ARTICLE

Hen egg white lysozyme fibrillation: a deep-UV resonance Raman spectroscopic study

Ming Xu[1], *Vladimir V. Ermolenkov*[1], *Vladimir N. Uversky*[2], *and Igor K. Lednev*[1]

[1] Department of Chemistry, University at Albany, SUNY, 1400 Washington Ave., Albany, NY 12222, USA
[2] Center for Computational Biology and Bioinformatics, Department of Biochemistry and Molecular Biology, Indiana University School of Medicine, Indianapolis, 714 North Senate Ave., Suite 250, IN 46202, USA and Institute for Biological Instrumentation, Russian Academy of Sciences, Pushchino, Moscow Region 142292, Russia

Received 13 October 2007, revised 11 December 2007, accepted 12 December 2007
Published online 14 February 2008

Key words: Hen egg white lysozyme; deep-UV resonance Raman spectroscopy; tryptophan fluorescence spectroscopy; circular dichroism spectroscopy; amyloid fibril; fibrillation

PACS: 33.55.Ad, 87.64.Je, 87.64.Ni

Amyloid fibrils are associated with numerous degenerative diseases. The molecular mechanism of the structural transformation of native protein to the highly ordered cross-β structure, the key feature of amyloid fibrils, is under active investigation. Conventional biophysical methods have limited application in addressing the problem because of the heterogeneous nature of the system. In this study, we demonstrated that deep-UV resonance Raman (DUVRR) spectroscopy in combination with circular dichroism (CD) and intrinsic tryptophan fluorescence allowed for quantitative characterization of protein structural evolution at all stages of hen egg white lysozyme fibrillation *in vitro*. DUVRR spectroscopy was found to be complimentary to the far-UV CD because it is (i) more sensitive to β-sheet than to α-helix, and (ii) capable of characterizing quantitatively inhomogeneous and highly light-scattering samples. In addition, phenylalanine, a natural DUVRR spectroscopic biomarker of protein structural rearrangements, exhibited substantial changes in the Raman cross section of the 1000-cm^{-1} band at various stages of fibrillation.

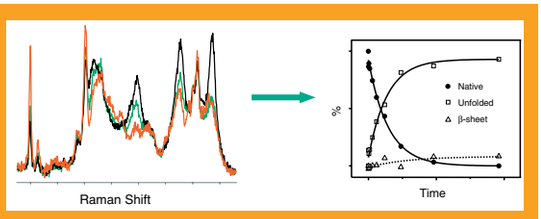

The kinetics of the structural evolution during hen egg white lysozyme fibrillation characterized by deep-UV resonance Raman spectroscopy.

J. Biophoton. 1, No. **3**, 215–229 (2008) / **DOI** 10.1002/jbio.200710013

WILEY-VCH

REPRINT

J. Biophoton. **1**, No. 3, 215–229 (2008) / **DOI** 10.1002/jbio.200710013

Journal of BIOPHOTONICS

FULL ARTICLE

Hen egg white lysozyme fibrillation: a deep-UV resonance Raman spectroscopic study†

Ming Xu[1], *Vladimir V. Ermolenkov*[1], *Vladimir N. Uversky*[2], *and Igor K. Lednev*[1,*]

[1] Department of Chemistry, University at Albany, SUNY, 1400 Washington Ave., Albany, NY 12222, USA
[2] Center for Computational Biology and Bioinformatics, Department of Biochemistry and Molecular Biology, Indiana University School of Medicine, Indianapolis, 714 North Senate Ave., Suite 250, IN 46202, USA and Institute for Biological Instrumentation, Russian Academy of Sciences, Pushchino, Moscow Region 142292, Russia

Received 13 October 2007, revised 11 December 2007, accepted 12 December 2007
Published online 14 February 2008

Key words: Hen egg white lysozyme; deep-UV resonance Raman spectroscopy; tryptophan fluorescence spectroscopy; circular dichroism spectroscopy; amyloid fibril; fibrillation

PACS: 33.55.Ad, 87.64.Je, 87.64.Ni

Amyloid fibrils are associated with numerous degenerative diseases. The molecular mechanism of the structural transformation of native protein to the highly ordered cross-β structure, the key feature of amyloid fibrils, is under active investigation. Conventional biophysical methods have limited application in addressing the problem because of the heterogeneous nature of the system. In this study, we demonstrated that deep-UV resonance Raman (DUVRR) spectroscopy in combination with circular dichroism (CD) and intrinsic tryptophan fluorescence allowed for quantitative characterization of protein structural evolution at all stages of hen egg white lysozyme fibrillation *in vitro*. DUVRR spectroscopy was found to be complimentary to the far-UV CD because it is (i) more sensitive to β-sheet than to α-helix, and (ii) capable of characterizing quantitatively inhomogeneous and highly light-scattering samples. In addition, phenylalanine, a natural DUVRR spectroscopic biomarker of protein structural rearrangements, exhibited substantial changes in the Raman cross section of the 1000-cm^{-1} band at various stages of fibrillation.

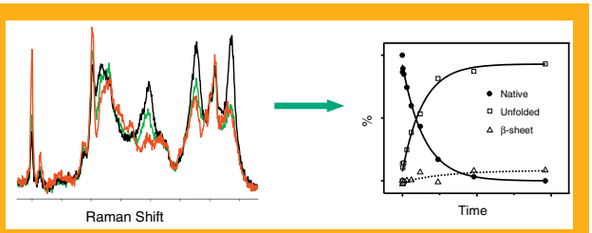

The kinetics of the structural evolution during hen egg white lysozyme fibrillation characterized by deep-UV resonance Raman spectroscopy.

© 2008 by WILEY-VCH Verlag GmbH & Co. KGaA, Weinheim

1. Introduction

Amyloid fibrils are associated with numerous debilitating diseases such as Alzheimer's disease (AD), Parkinson's disease (PD), Huntington's diseases (HD), prion disease, familial amyloid polyneuropathy (FAP), senile systemic amyloidosis and type II diabetes, etc [1–4]. Specific protein/peptide are associated with certain diseases. For instance, Aβ peptide and hyperphosphorylated tau protein are found in

* Corresponding author: e-mail lednev@albany.edu, Phone: +00 1 518 591 8863, Fax: +00 1 518 442 3462
† Preliminary results of this study have been published elsewhere (Biopolymers, **79**, 58–61 (2005)).

WILEY InterScience® DISCOVER SOMETHING GREAT

© 2008 by WILEY-VCH Verlag GmbH & Co. KGaA, Weinheim

the amyloid plaques of the AD patients; ubiquinated α-synuclein is found in the Lewy bodies of PD patients and huntingtin with N-terminal polyglutamine expansion deposits is found in the HD patients, etc. [4, 5]. Other proteins, such as lysozyme, [6, 7] immunoglobulin light chain [8–11] and β-2 microglobulin [12–14] are associated with amyloidosis that affect mainly peripheral organs. Further, even proteins that are not associated with any degenerative diseases are transformed into amyloid fibrils *in vitro*, among them are α-lactalbumin, [15, 16] insulin [17, 18] and myoglobin [19]. Most fibrillogenic proteins have no structural similarity in their native form: they may be largely β-sheet or α-helix or a mixture of both, as well as "natively unfolded" [20]. Large genetically engineered polypeptides with a simple repetitive primary sequence are able to form fibrils under certain conditions as well [21–23].

Despite the diversity in the primary sequence of the fibrillogenic proteins, the fibrils adopt a common structure – straight, nonbranching fibers with a diameter of about 7–12 nm and lengths ranging from 100 nm to tens of micrometers [24, 25]. X-ray fiber diffraction showed that the fibrils possess a unique cross-β structure, in which β-strands arrange in parallel or antiparallel fashion between each other and perpendicular to the long axis of the fibril [25, 26]. The favorable hydrophobic interactions are maximized while the unfavorable electrostatic interactions in the protofilament core are avoided in this arrangement [27].

There is evidence that the accumulation of amyloid fibrils is the major culprit of the slowly progressive neurodegenerative disorders [3, 4, 28]. Since the amyloid fibrils are exceptionally stable once formed, to prevent their formation might be a promising strategy in finding the cure for the devastating diseases. The partially folded intermediate is also postulated to be harmful to cells [28, 29]. Therefore, it could be beneficial to understand the early events of the fibrillation process.

It has been shown in many *in-vitro* studies that destabilization of the native structure can promote the formation of amyloid fibrils. Among the destabilization conditions are: mutation [7, 20, 30, 31], addition of alcohol [32–37], denaturation [18, 38], reduction [36, 39], incubation of acidic solution at high temperature [40–43], etc. Biophysical techniques such as NMR [31, 39, 44–47], small angle X-ray/neutron scattering (SAXS/SANS) [34, 37, 48, 49], thioflavin T (ThT) fluorescence [6, 15, 50–52], circular dichroism (CD) spectroscopy [38, 42, 47, 53], FTIR [37, 47, 54], static/dynamic light scattering [42, 55–57], etc. have been applied to study the fibrillation process *in vitro*. Based on these studies, several kinetic and thermodynamic mechanisms involving a number of steps and intermediate states have been suggested for amyloid fibril formation [1, 3, 58]. *What is lacking at the moment is a quantitative characterization of protein structural rearrangements at every stage of fibrillation*. This is because the macroscopic properties of an amyloidogenic protein solution change during the fibrils formation *in vitro*: a gelatinous phase appears, which is mainly composed from fibrils [59]. The insoluble phase poses a serious problem in applying conventional biophysical techniques for studying protein structural transformations during the fibril formation. Raman spectroscopy, by its nature, is based on inelastic light scattering [60] and can be utilized equally well for both transparent and highly light-scattering samples [59, 61, 62]. When the incident light interacts with a molecule, the scattered photons might lose energy due to the excitation of molecular vibrations. The analysis of the scattered photons gives a vibrational signature of the scattering molecule, providing rich structural information. In addition, when the energy of the incident light falls within an electronic transition, the Raman scattering is greatly enhanced due to the resonance effect. For instance, UV Raman spectroscopy is used to study protein folding/unfolding by examining the transition of both secondary [63, 64] and tertiary [65] structures. Specifically, the resonance enhancement of the vibrational modes from an amide chromophore (a building block of the polypeptide backbone) provides information on the evolution of protein secondary structure [66]. The vibrational modes of aromatic amino acid side chains, specifically phenylalanine and tyrosine, are resonantly enhanced when deep-UV excitation is used, providing information on the evolution of the tertiary structure [66]. More detailed information on protein secondary structure, such as the distribution of polypeptide backbone dihedral angles, can also be derived from protein deep-UV Raman spectra [67].

In this work, the *in-vitro* amyloid fibril formation of hen egg white lysozyme (herein refer to as lysozyme) was studied *quantitatively* using deep-UV resonance Raman (DUVRR) spectroscopy with an excitation of 197 nm, along with other spectroscopic techniques including tryptophan fluorescence and far-UV circular dichroism (CD). Hen egg white lysozyme was chosen because the structural properties and the folding/unfolding behavior of lysozyme have been studied extensively over recent decades [68–70]. Well-accumulated data on lysozyme structure and the ability to form amyloid fibrils *in vitro* make this protein an excellent model for studying protein structural transition during fibril formation. We found that an *irreversible* partial unfolding was the first step of lysozyme amyloid fibril formation.

Both secondary and tertiary structural transitions of lysozyme at the early stages of fibrillation were quantitatively characterized. For the secondary structure characterization, since we are mainly interested in the α-helix and β-sheet contributions, we categor-

© 2008 by WILEY-VCH Verlag GmbH & Co. KGaA, Weinheim

ize the rest of the protein conformations as disordered structures. According to a modern viewpoint, a "truly disordered" or random coil conformation can be found very rarely for a protein or polypeptide chain. Instead, a polyproline II conformation (PPII) and various turns dominate. Consequently, an alternative term for the disordered structure, which is often used in recent literature, would be "other structures." It was found that the unfolding mainly involved the melting of α-helix into the disordered structures. The native lysozyme, which consists of 32% of α-helix, [71] unfolded irreversibly into a partially folded intermediate containing 6% of α-helix before it assembled into fibrils. The quantification of the secondary structure using far-UV CD and DUVRR spectra of protein were compared. The changes in the lysozyme tertiary structure were followed using tryptophan fluorescence and DUVRR spectroscopic signature of phenylalanine. The sensitivity of the ν_{12} vibrational mode of phenylalanine, the intrinsic DUVRR spectroscopic biomarker, to the local environment, was verified using *N*-acetyl-L-phenylalanine ethyl ester in a water-acetonitrile solution as a model system. Both secondary and tertiary structure of lysozyme was found to unfold monoexponentially during the incubation with the characteristic time of ~30 h.

2. Experimental

2.1 Materials

Hen egg white lysozyme, poly(L-glutamic acid) (PGA, MW = 49 000), poly(L-lysine) (PLL, MW = 28 200), trifluoroethanol, sodium trifluoroacetate, guanidine hydrochloride (GdHCl), EDTA, dithiothreitol (DTT), *N*-acetyl-L-phenylalanine ethyl ester (ac-phe-ee), acetonitrile (spectrophotometric grade), Sephadex G-25 superfine was purchased from Sigma-Aldrich (St. Louis, MO USA) and used as received.

2.2 In-vitro fibril formation of lysozyme

The method described by Krebs et al. [40] was utilized for *in-vitro* fibril formation. The Lysozyme solution (14 mg/ml, pH 2.0 adjusted by adding HCl) was incubated at 65 °C. The incubation was terminated after various durations; gelatinous fraction was separated by centrifugation at 16 000 g for 30 min at room temperature. Both fractions, supernatant and gelatinous phase, were characterized separately. The Lysozyme concentration in the solution fraction was determined by UV absorption using a Hewlett-Packard 8452A photodiode array spectrophotometer. Lysozyme was denatured in 6 M GdHCl before the UV absorption measurement. $\varepsilon_{280\ \mathrm{nm}} = 33\,882\ \mathrm{L\ mol^{-1}\ cm^{-1}}$ was used to calculated the concentration [36, 72].

2.3 Preparation of denatured-reduced lysozyme

The denatured-reduced lysozyme was prepared following the procedure reported by Cao et al. [36] with minor modifications. The denaturing-reducing buffer consisted of 0.1 M Tris-HCl, 1 mM EDTA, 7 M GdHCl and 0.27 M DTT at pH 8.6. The buffer was deoxygenated by bubbling nitrogen gas. Lysozyme was dissolved in the above buffer to the final concentration of ~18 mg/ml. The protein solution was sealed, vacuumed and then protected with nitrogen gas. The container was wrapped by aluminum foil and held at room temperature for 24 h. The reducing reaction was stopped by adjusting the pH to 3.0 using acetic acid. The solution was filtered through a Sephadex G-25 superfine column pre-equilibrated with 100 mM acetic acid. Elution fractions were collected and monitored by absorbance at 280 nm. Fractions at the first elution peak were pooled and dialyzed against pH 3.0 HCl solution for 24 h under the protection of nitrogen gas. The protein concentration was determined by diluting the protein solutions in 6 M guanidine hydrochloride solution and measuring the UV absorbance at 280 nm.

2.4 Atomic force microscope (AFM) imaging of lysozyme fibrils

The gelatinous phase of the incubated lysozyme collected by centrifugation was resuspended in pH 2.0 HCl solution with a 1 : 400 dilution factor (V: V) and treated in an ultrasonic bath for 15 min. The fibril suspension was then deposited onto freshly cleaved mica supports and incubated for 2 min followed by washing in deionized water and dried by nitrogen gas. The AFM imaging was performed on a NTEGRA spectra Raman spectroscopy SPM system (NT-MDT Co., Russia), in semicontact mode. Supersharp DLC silicon probes were used (nsg01-dlc: resonant frequency 150 kHz, stiffness 5 N/m). The initial amplitude of cantilever oscillations was in the range of 3–7 nm. The setpoint was chosen at the attractive regime of tip-sample interaction.

© 2008 by WILEY-VCH Verlag GmbH & Co. KGaA, Weinheim

2.5 Tryptophan fluorescence spectroscopy

The soluble fractions of the incubated lysozyme samples were diluted in pH 2.0 HCl solution to final absorption of no more than 0.05 at a 1 cm path length for the tryptophan fluorescence spectroscopic measurements. The tryptophan fluorescence spectra were measured using a PerkinElmer LS 55 luminescence spectrometer. The excitation wavelength was 280 nm. The slits for both excitation and emission were 5.0 nm.

2.6 Far-UV CD spectroscopy

Far-UV CD (190–250 nm) spectra of lysozyme were measured using a JASCO J-810 spectropolarimeter at room temperature. For protein concentrations of ~1 mg/ml, a 0.02 cm path length cell was used. The CD spectra were acquired with 50 nm/min scan speed at 1 nm step and 2.0 nm bandwidth. Three spectra were accumulated and averaged for each sample. Protein secondary structure composition was evaluated using CDPro software package [73]. The CDPro software package contains three programs for the secondary structure determination from the far-UV CD spectra: SELCON3 [74], CDSSTR [75] and CONTIN [76]. The fitting results from all three programs were averaged.

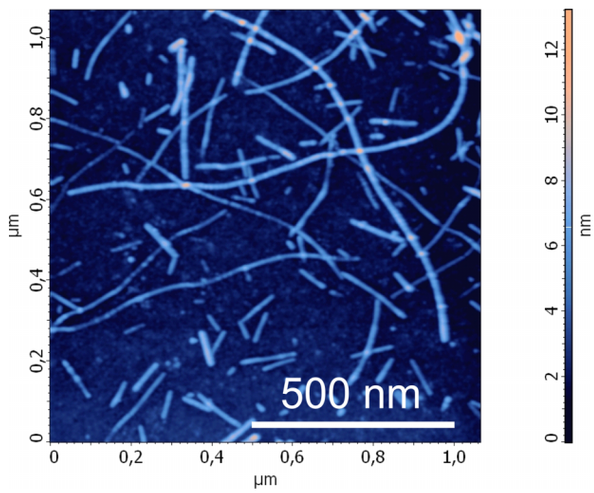

Figure 1 (online colour at: www.biophotonics-journal.org) AFM image of lysozyme fibrils measured in air. Lysozyme solution (14 mg/ml, pH 2.0) was incubated at 65 °C. The gelatinous fraction was collected by centrifugation at 16 000 g for 30 min and resuspended in pH 2.0 HCl solution with a 1 : 400 dilution factor (V : V) and treated in an ultrasonic bath for 15 min. The fibril suspension was then deposited onto freshly cleaved mica supports and incubated for 2 min followed by washing in deionized water and dried by nitrogen gas. The AFM imaging was performed on a NTEGRA Raman spectroscopy SPM system (NT-MDT Co., Russia) in semicontact mode.

2.7 Deep-UV resonance Raman (DUVRR) spectroscopy

197 nm excited DUVRR spectra were measured using a home-built Raman spectrometer as described elsewhere [43]. A spinning NMR tube with a magnetic stirrer inside was used for sampling. GRAMS/AI 7.0 (Thermo Galactic, Salem, NH) was used for data processing. Lysozyme solutions with 1–14 mg/ml protein were normally used for DUVRR measurements. Sodium trifluoroacetate (TFA) was used as an internal standard for spectral normalization purpose where appropriate. The DUVRR spectra of protein solutions with and without TFA showed that the addition of this internal standard did not alter the lysozyme DUVRR spectra (data not shown).

3. Results

3.1 Spectroscopic characterization of lysozyme at various stages of fibrillation

3.1.1 Atomic force microscopy

Lysozyme solution (pH 2.0) incubated at 65 °C for prolonged time formed a gelatinous phase that can be separated by centrifugation. AFM was utilized for a direct visual inspection of the separated insoluble phase. As shown in Figure 1, the insoluble phase consists of nonbranched fibers in various lengths with an average height of 3–6 nm. This is in agreement with other AFM results reported for lysozyme fibrils [42, 77].

3.1.2 Tryptophan fluorescence

Tryptophan is often used as a natural fluorescence marker for characterizing protein tertiary structural changes [78]. Figure 2 shows the fluorescence spectra of lysozyme (dominated by the contribution from 6 tryptophan residues) obtained before and after eight-day incubation. Both spectra were measured at room temperature. The red-shifted peak of the tryptophan fluorescence spectra indicated that the tryptophan side chains in the unfolded lysozyme were exposed to the aqueous environment more than that in the native protein [78]. Therefore, prolong incuba-

© 2008 by WILEY-VCH Verlag GmbH & Co. KGaA, Weinheim

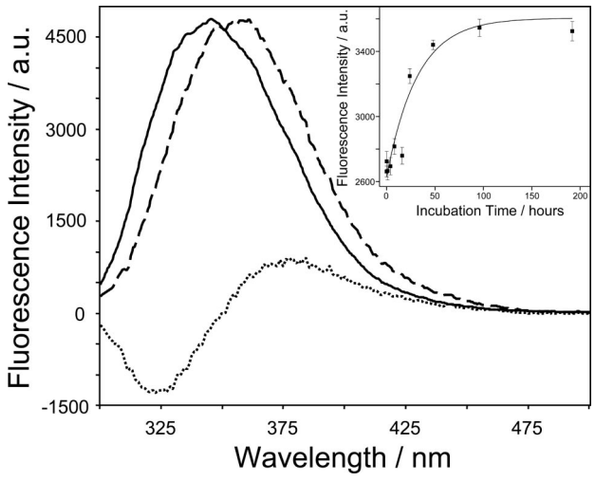

Figure 2 Tryptophan fluorescence spectra of nonincubated (solid), the solution phase of 8-day-incubated lysozyme (dashed line) and the difference spectrum of the above two spectra (dotted line). The inset shows the change in the fluorescence intensity at 379 nm with the incubation time.

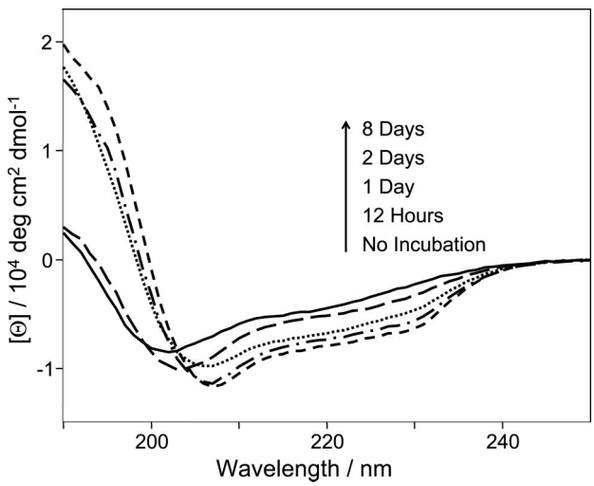

Figure 3 Far-UV CD spectra of the solution phase of lysozyme samples incubated at 65 ºC for various times (from bottom up: short dashed line: nonincubated lysozyme; dotted-and-dashed line: 12-h-incubated; dotted line: 1-day-incubated; long-dashed line: 2-day-incubated and solid line: 8-day-incubated lysozyme). The arrow indicates the increasing of incubation time. The spectra were measured at room temperature shortly after the incubation.

tion of lysozyme resulted in the disruption of the protein tertiary structure. To evaluate the kinetics of the tertiary structural changes, the intensity of lysozyme fluorescence at 379 nm was plotted as a function of the incubation time (Figure 2, Inset). This particular wavelength was chosen because it corresponds to the maximum in the difference spectrum (Figure 2, dotted spectrum). The kinetic data were found to fit well to the monoexponential function with a characteristic time of 32 ± 4 h.

3.1.3 Far-UV CD spectroscopy

Room-temperature far-UV CD spectra of the solution fractions of lysozyme incubated at 65 °C for various times are shown in Figure 3. A progressive decrease in the α-helix contribution with the incubation time is evident from the spectra. The molar ellipticity values reported in Figure 3 were calculated based on lysozyme concentrations estimated by UV absorption spectroscopy.

3.1.4 DUVRR spectroscopy

Both supernatant and gelatinous phases of the incubated lysozyme were characterized separately by DUVRR spectroscopy. DUVRR spectra of lysozyme measured at various stages of fibrillation are shown in Figure 4. The contributions from amide chromophore and aromatic amino acid side chains, mainly phenylalanine and tyrosine, dominated the 197 nm excited Raman spectra. The DUVRR signature of

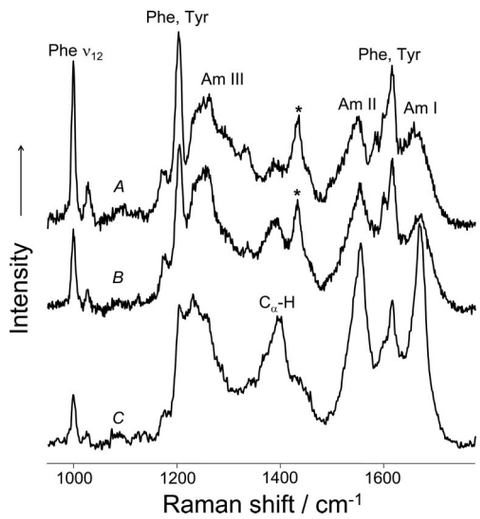

Figure 4 197 nm excited Raman spectra of the nonincubated lysozyme (A), soluble phase of 2-day-incubated lysozyme (B), and the gelatinous phase (C). 14 mg/ml lysozyme solution (pH 2.0) was incubated at 65 °C. The incubation was terminated after the indicated time points and the solution fraction was separated from the gelatinous fraction by centrifugation at 16000 g for 30 min. Trifluoroacetate (TFA) was used as an internal standard for the soluble lysozyme (TFA band is marked with the asterisk).

© 2008 by WILEY-VCH Verlag GmbH & Co. KGaA, Weinheim

the amide chromophore consists of amide I, amide II, amide III and C_α–H bending bands that report on the protein secondary structure [60, 63]. Amide I mode (Am I) consists of carbonyl C=O stretching, with a small contribution from C–N stretching and N–H bending. Amide II and Amide III bands involve significant C–N stretching, N–H bending, and C–C stretching. The C_α–H bending vibrational mode involves C_α–H symmetric bending and C–C_α stretching [63]. The DUVRR spectra for the solution phase of the incubated lysozyme changed gradually with the incubation: the intensity of C_α–H band (1390 cm^{-1}) and amide II band increased, and the frequency of amide II band upshifted (Figure 4). These changes indicated α-helix melted into disordered structures [63,79]. The amide III band (around 1250 cm^{-1}), being the most complex band, showed an increase of the intensity in the 1270–1320 cm^{-1} region and a small decrease in the 1230–1270 cm^{-1} region. The increased, upshifted and sharpened amide I band after two days of incubation (Figure 4) indicated the formation of β-sheet conformation.

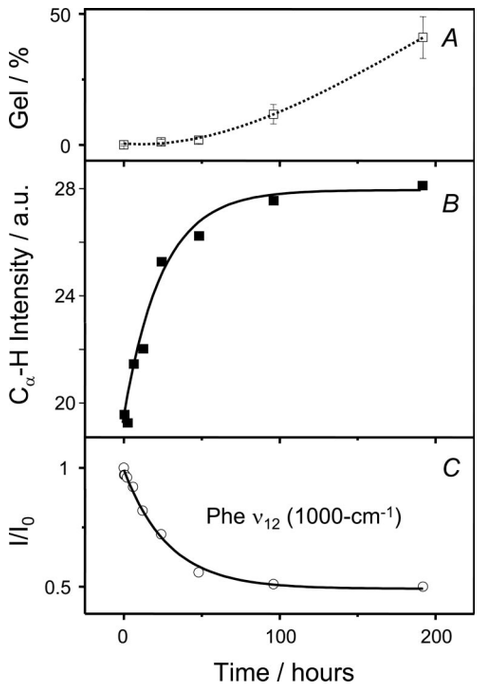

Figure 5 (A) The fraction of lysozyme deposited into the insoluble phase, which was determined from the decrease in the protein concentration in the solution phase separated by centrifugation. (B) The change in the intensity of the C_α–H Raman band of lysozyme with the incubation time. (C) The relative intensity of the 1000 cm^{-1} phenylalanine Raman band of lysozyme solutions incubated for various times. Trifluoroacetate (TFA) was used as an internal standard: the 1000 cm^{-1} phenylalanine Raman band was normalized against the TFA band at 1435 cm^{-1}. I_0 corresponds to the relative band intensity in the spectrum of a nonincubated solution. I values were normalized to the protein concentration in solution phase.

The formation of the gelatinous phase had a lag time of about 2 days (Figure 5A), which is consistent with an earlier report [42]. The DUVRR spectrum of the insoluble phase, dominated by fibrils, showed a distinctively different spectrum as compared with the spectra of the soluble phase (Figure 4). DUVRR spectrum of lysozyme fibrils comprised sharp and intense amide I and amide II bands and a greatly increased C_α–H band. The aromatic bands derived from phenylalanine and tyrosine side chains were all decreased substantially in comparison with the amide bands (Figure 4).

The phenylalanine ν_{12} vibrational mode (1000 cm^{-1}) decreased dramatically in the DUVRR spectra of incubated lysozyme samples (Figure 4). Figure 5C showed the time dependence of the intensity of phenylalanine 1000 cm^{-1} band: the intensity decreased monoexponentially with the incubation with a characteristic time of 29 ± 2 h. Following Spiro and coworkers' earlier report [80], one could hypothesize that the intensity of the phenylalanine 1000 cm^{-1} Raman band decreased with the incubation time due to lysozyme denaturation and the exposure of phenylalanine to water. In order to test this hypothesis we investigated the dependence of the Raman cross section of *N*-acetyl-L-phenylalanine ethyl ester (ac-phe-ee) on solvent composition.

3.2 Phenylalanine is a natural DUVRR spectroscopic probe of local environment

DUVRR spectra of ac-phe-ee excited with 197 nm laser were measured in acetonitrile-water solutions with various solvent compositions (Figure 6). Acetonitrile, a solvent of moderate polarity, was chosen because it is miscible with water and it was "transparent" at 197 nm. Two sets of samples were prepared in order to encompass both high and low contents of acetonitrile: (a) a 1.17 mM ac-phe-ee solution in acetonitrile was diluted with various amounts of water to obtain solvent compositions with acetonitrile content varied from 5% to 100%. Acetonitrile was used as an internal standard to normalize the Raman spectra of ac-phe-ee; (b) Up to 6% of acetonitrile was added to 0.20 mM ac-phe-ee solution in water containing 100 mM $NaClO_4$. Perchlorate was used as the internal standard in this set of ac-phe-ee Raman spectral measurements. No photodegradation was evident for the samples at the laser (197 nm) output power of 0.5 mW, which corresponded to an irradiating power of ~0.2 mW at samples [43].

© 2008 by WILEY-VCH Verlag GmbH & Co. KGaA, Weinheim

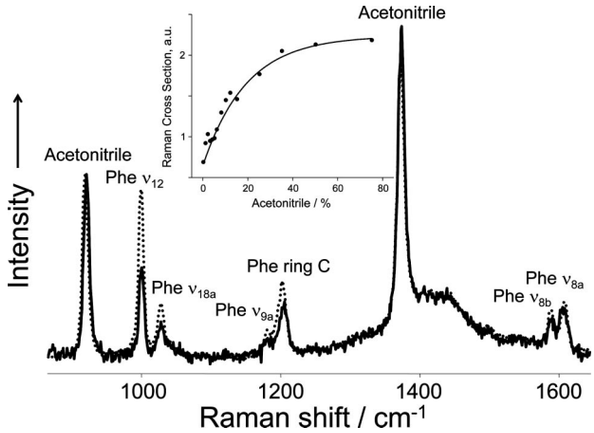

Figure 6 197 nm excited resonance Raman spectra of *N*-acetyl-L-phenylalanine ethyl ester (ac-phe-ee) in aqueous solution containing 50% (dotted line) and 5% (solid line) of acetonitrile. Inset: The effect of the solvent composition on the Raman cross section of the phenylalanine ν_{12} vibrational mode.

The obtained Raman spectra (Figure 6) consisted of two sharp acetonitrile bands (918 cm^{-1} and 1374 cm^{-1}) and six prominent bands from ac-phe-ee, which can be assigned to the phenyl ring: ν_{12} (ring stretching, 1000 cm^{-1}), ν_{18a} (inplane C–H bending, 1028 cm^{-1}), ν_{9a} (inplane C–H bending, 1182 cm^{-1}), ring-C (phenyl-C stretching, 1204 cm^{-1}) and the in-plane ring-stretching doublet ν_{8b} (1589 cm^{-1}) and ν_{8a} (1608 cm^{-1}) [81, 82]. The Raman cross section of the ν_{12} phenyl vibrational mode (1000 cm^{-1}) increased monotonically with increasing acetonitrile content and reached saturation at ~50% acetonitrile (Figure 6, inset). The obtained results supported the above hypothesis that the phenylalanine 1000 cm^{-1} DUVRR cross section decreases with the increase in water exposure. Consequently, phenylalanine is a natural DUVRR spectroscopic probe of the local environment and can be used for characterizing the changes in protein tertiary structure.

3.3 The first step of lysozyme fibrillation, partial unfolding, is a completely irreversible process

Partial unfolding of fibrillogenic proteins is believed to be the first step toward fibril formation [20]. A mutational study using protein G B1 variants also suggests that it is the overall stability rather than the specific destabilizing mutation that facilitates the amyloid fibril formation [83]. Unlike its structural cousin α-lactalbumin, which adopts a molten globule state (protein tertiary structure is disrupted while the secondary structure is largely preserved) when acidified [15], lysozyme is very stable: lowering the pH to 2.0 has no effect on the structure of lysozyme as examined by DUVRR spectroscopy (data not shown), although it has been reported that lysozyme tertiary structure is disrupted at pH 1.5. [84].

The changes in lysozyme fluorescence and far-UV CD spectra reported above (Figures 2 and 3) for the solution part of incubated protein were measured at room temperature. This indicated at least partial irreversibility of the unfolding process induced by the prolonged thermal treatment of the protein. DUVRR spectroscopy was used to quantify the extent of irreversibility. Figure 7 shows the DUVRR spectra of lysozyme measured (i) at 65 °C after incubating for 24 h and (ii) at room temperature (24 °C) shortly after the incubation. The spectra were very similar to each other (and quite different from the spectrum of native lysozyme). This result indicated a complete irreversible character of the structural rearrangements, mainly α-helix melting, during prolonged incubation at elevated temperature. In contrast, completely reversible α-helix melting has been reported for relatively brief heating of lysozyme [43]. A small difference between the two spectra (difference spectrum in Figure 7) can be attributed to the dependence on temperature. The noiseless spectrum in Figure 7 represents the temperature dependence of the random coil Raman spectrum of a polypeptide (mainly alanine, without aromatic residues, adopted from ref. [85]). There are also small contributions from phenylalanine and ty-

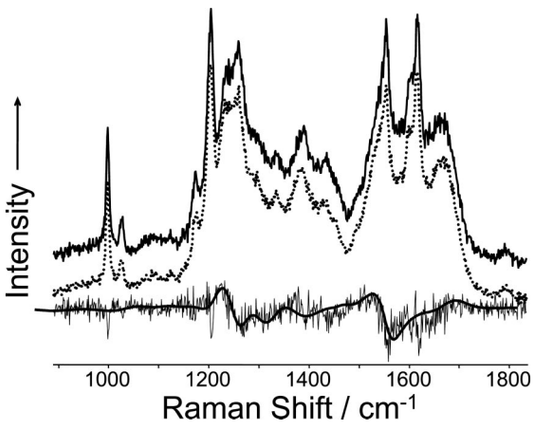

Figure 7 DUVRR spectra of the solution phase of the 24-h-incubated lysozyme (at 65 °C) measured at 65 °C (top, solid line) and 24 °C (middle, dotted line). The two spectra are shifted to aid clarity. Also shown is the difference spectrum (bottom, solid line, noisy spectrum). The bottom noiseless spectrum overlapping with the difference spectrum represents the temperature dependence of the random-coil spectrum for a temperature difference of 40 °C, adopted from Lednev et al. [85].

© 2008 by WILEY-VCH Verlag GmbH & Co. KGaA, Weinheim

Journal of
BIOPHOTONICS

rosine in the difference spectrum (Figure 7). Since the Raman spectrum of phenylalanine is temperature independent [43], it is plausible to suggest that the local environment around phenylalanine and tyrosine residues are different at 65 °C and 24 °C. Tentatively, the lysozyme may adopt a "loose" tertiary conformation at higher temperature while the secondary structure remains the same – an analog to the molten globule state. Further study utilizing dynamic light scattering for size characterization of lysozyme is underway in our laboratory to test this hypothesis.

3.4 Quantitative analysis of lysozyme structural rearrangements at early stages of fibrillation

One of our ultimate goals was to describe quantitatively the structural evolution of lysozyme during the fibril formation. In our previous report [59], the linear combination of three spectra corresponding to the native lysozyme, the partially unfolded intermediate and the fibrils (mainly β-sheet conformation) was used to fit the DUVRR spectra of the soluble fractions of lysozyme incubated for various durations (Figure 8). The contribution of the native conformer decreased and the content of the unfolded conformer increased in a monoexponential manner with a characteristic time of 28 ± 2 h. The contribution of a newly formed β-sheet gradually reached about 8% after 4 days of incubation (Figure 8). In this study, we compared the application of two methods, DUVRR and far-UV CD spectroscopy, for quantitative characterization of protein secondary structure changes at early stages of lysozyme fibrillation.

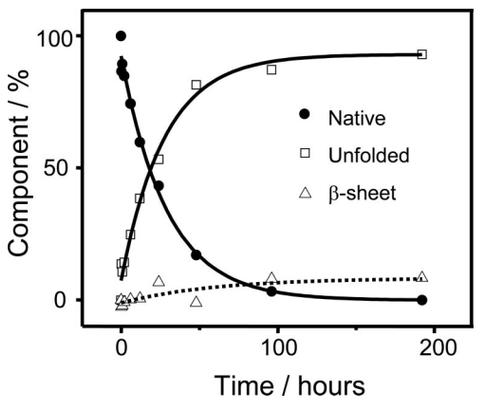

Figure 8 The evolution of the composition of different lysozyme conformers in the soluble fractions of the incubated samples. DUVRR spectra of the solution phase of incubated lysozyme were fitted with a linear combination of DUVRR spectra for native, partially unfolded (the solution phase of 8 days incubated lysozyme) and the fibrils of lysozyme.

Table 1 Secondary structure contents of the solution phase from incubated lysozyme determined by far-UV CD spectroscopy.

Time, h	α-helix	β-sheet	Disordered structures
0	34%	18%	48%
6	33%	19%	47%
12	31%	21%	46%
24	22%	25%	52%
48	15%	29%	55%
96	11%	29%	57%
192	8%	32%	57%
Native Lysozyme*	32%	6%	62%

* The secondary structural composition of native lysozyme determined by X-ray crystallography (PDB ID 1BHZ) [71].

The soluble fractions of the incubated lysozyme were separated and characterized by far-UV CD spectroscopy (Figure 3). The secondary structure composition at different incubation times was estimated using the CDPro software [73] (Table 1). The contribution of β-sheet (18%) to the native lysozyme was overestimated relative to the X-ray data (6%) [71]. A further increase in β-sheet content by 14% as a result of the prolonged incubation was also overestimated, as is evident from the Raman spectroscopic data (see below). Far-UV CD spectroscopy is well known to be more selective and sensitive to the α-helix than to the β-sheet and the disordered structures [86]. Consequently, it is not surprising that far-UV CD spectroscopic analysis misestimated the contribution from β-sheet while the α-helix content was estimated quite accurately.

The DUVRR spectroscopic signature of β-sheet is very distinctive: it consists of strong amide I, amide II and C_α–H bands (Figure 4C). In addition, the amide I band of β-sheet is sharper, which differentiates itself from that of α-helix and disordered structures. For instance, the Raman cross section (which is proportional to the band intensity) of amide I bands for α-helix, β-sheet and random coil reported by Huang et al. [64] are 52, 217 and 178 (in relative units), respectively. Therefore, one would expect a much larger amide I intensity in the DUVRR spectrum of 2-day-incubated lysozyme (Figure 4B) in the case of the 11% increase of β-sheet suggested by far-UV CD (Table 1). There were, however, only a slight shift in the amide I band in the DUVRR spectrum of 4-day-incubated lysozyme, which signifies a very small percentage of β-sheet contribution.

© 2008 by WILEY-VCH Verlag GmbH & Co. KGaA, Weinheim

3.5 Basis DUVRR spectra of secondary structural elements

Quantitative analysis of Raman spectroscopic data, the evaluation of protein secondary structure in particular, requires knowledge of basis spectra of secondary structural elements. Several different sets of far-UV CD spectra have been reported and used for characterizing the secondary structure of proteins and polypeptides [73]. Various approaches for obtaining DUVRR basis spectra have also been utilized. First, statistical analysis of Raman spectra recorded for a number of proteins with known secondary structural composition allowed the averaged spectroscopic signatures of main secondary structural elements to be obtained [63, 64]. Second, homopolypeptides forming one predominant conformation under certain conditions were used for measuring the spectroscopic signature of this conformation. Both these approaches have certain limitations because a DUVRR spectrum depends on the polypeptide/protein primary sequence. "Perfect" basis spectra were obtained for an oligopeptide by generating the conformation with a single predominant secondary structure for the oligopeptide itself [85].

Two sets of basis DUVRR spectra for protein secondary structural elements were obtained in this study. First, the basis DUVRR spectra of α-helix, β-sheet and disordered structures were found using homopolypeptides as described by Chi et al. [63] In particular, the disordered structures spectrum was acquired using a pH 7.1 PGA solution at 23 °C. The α-helix spectrum was measured using a pH 4.3 PGA solution at 0 °C. PLL was dissolved in water (pH 11.3) and then incubated at 52 °C for 3 h to prepare the β-sheet-rich conformation. The application of this set of basis spectra for fitting the lysozyme spectra measured at early stages of incubation was not satisfactory (data not shown). There is a serious disadvantage in using homopolypeptide basis spectra for proteins because DUVRR spectra depend on the primary sequence. Therefore, we obtained the second set of basis Raman spectra of lysozyme by converting the protein into a single predominant secondary structural conformation. Lysozyme was denatured and reduced to model the unordered conformation using a reported method [36, 57]. Trifluoroethanol (TFE) was used to induce the α-helical conformation [32, 51, 87]. Figure 10 shows DUVRR spectra of the denatured-reduced lysozyme in aqueous solution and that containing 30% TFE. The secondary structural composition of the denatured-reduced lysozyme in the presence of TFE was estimated based on far-UV CD data using CDPro software package (Table 2). The CD spectra of lysozyme (Figure 9) showed a typical disordered structures $\rightarrow$ α-helix transition with increasing TFE content.

The native lysozyme, which contains 32% of α-helix and 62% of disordered structures based on X-ray crystallography data [71], was denatured and reduced into a largely disordered structure (Figures 9 and 10). The secondary structural composition of the denatured-reduced lysozyme was 12% of α-helix, 16% of β-sheet and 72% of disordered structures, as estimated from far-UV CD data (Table 2). Upon addition of TFE, the random-coil-like far-UV CD spectra of the denatured-reduced lysozyme (single minimum at ~200 nm) changed gradually into α-helix-like spectra (dual minima at 207 nm and 222 nm, Figure 9). The α-helix content of the denatured-reduced lysozyme in 30% TFE solution was estimated to be 47%, which corresponds to a 35% increase from the 12% α-helix in the absence of TFE (Table 2). Higher concentrations (>30%) of TFE did

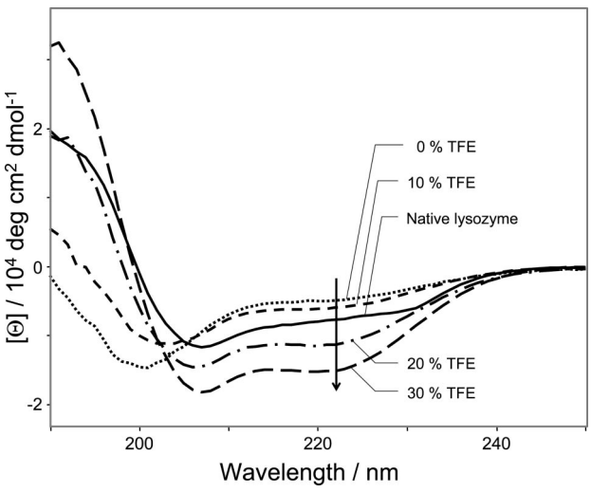

Figure 9 Far-UV CD spectra of denatured-reduced lysozyme in an aqueous solution containing various amounts of trifluoroethanol (TFE). From top down, denatured-reduced lysozyme in: water (dotted line), 10% (short-dashed line); 20% (dotted-and-dashed line) and 30% of TFE (long-dashed line). The far-UV CD spectrum of the native lysozyme is represented by the solid line. The arrow indicates the increasing negative ellipticity at 222 nm along with the increasing of TFE concentration.

Table 2 Secondary structure contents of denatured-reduced lysozyme in solvents with different TFE contents determined by far-UV CD spectroscopy.

Solvent	α-helix	β-sheet	Disordered structures
HCl, 1 mM	**12%**	16%	72%
10% TFE	17%	17%	65%
20% TFE	37%	7%	57%
30% TFE	**47%**	5%	48%

© 2008 by WILEY-VCH Verlag GmbH & Co. KGaA, Weinheim

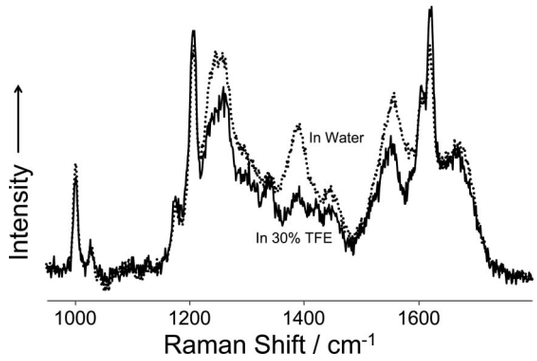

Figure 10 DUVRR spectra of denatured-reduced lysozyme in water (dotted line) and in 30% TFE (solid line). Lysozyme was denatured and reduced in a denaturing-reducing buffer consisted of 0.1 M Tris-HCl, 1 mM EDTA, 7 M GdHCl and 0.27 M DTT at pH 8.6 for 24 h at room temperature and subsequently purified by gel filtration (see Experimental, 2.3). Trifluoroacetate (TFA) was used as an internal standard and the TFA bands were subsequently subtracted from the spectra.

not result in any further noticeable increase in the α-helix spectral contribution.

The DUVRR spectra of denatured-reduced lysozyme in aqueous solution and that in the presence of 30% TFE are shown in Figure 10. The contribution from phenylalanine (1000 cm^{-1}, 1028 cm^{-1}, 1182 cm^{-1}, 1204 cm^{-1} and 1589 cm^{-1}/1608 cm^{-1} doublet) [81, 82] and tyrosine (1176 cm^{-1}, 1208 cm^{-1}, 1243 cm^{-1}, 1263 cm^{-1} and 1606/1621 cm^{-1} doublet) [81, 82] remained almost unchanged between the two spectra. At the same time, there were noticeable changes in amide II, amide III and C_α–H bending bands that were consistent with the formation of α-helix in the presence of TFE.

4. Discussion

4.1 Quantification of secondary structural transition

We attempted to quantitatively characterize the secondary structural transition of lysozyme during the fibril formation using a set of basis DUVRR spectra for secondary structural motifs obtained from homopolypeptide PLL and PGA. This approach, however, did not give satisfactory results. For instance, the DUVRR spectrum of lysozyme fibrils, which is predominantly cross-β structure, is significantly different from the β-sheet spectrum obtained from PLL (Figure 11A). This is not surprising since, for example, the DUVRR spectra of the disordered lysozyme and the disordered structures of PGA showed a large discrepancy especially in the region of C_α–H bending band (Figure 11B). The latter can be attributed to the heterogeneity of protein primary sequences in contrast to PGA.

Therefore, we made random-coil-rich and α-helix-rich conformers from lysozyme itself and measured DUVRR spectra for the two artificial conformers. Lysozyme was subjected to denaturation-reduction to generate artificial conformers with (i) enriched unordered structure and (ii) enriched α-helical conformation induced by TFE.

The secondary structural contents of denatured-reduced lysozyme in solution with different contents of TFE are shown in Table 2. The far-UV CD spectroscopic analysis of the lysozyme artificial conformers showed 11% in β-sheet content reduction when the denatured-reduced lysozyme was put into 30% TFE (Table 2). However, the DUVRR spectra did not indicate any noticeable change in the β-sheet content (Figure 10). In fact, the difference between DUVRR spectra of the denatured-reduced (random-coil-rich) and the α-helix-rich lysozyme conformations was very similar to the difference between PGA disordered structures and α-helix conformations (Figure 11C). The similarity suggested that, upon the addition of TFE, the α-helix formed mainly from unordered parts of denatured-reduced lysozyme with no noticeable melting of β-sheet.

On the other hand, far-UV CD spectroscopic analysis indicated the formation of 11% β-sheet in the soluble fraction of the lysozyme sample incubated for 4 days (Table 1). The increased contribution of the β-sheet in the 4-day-incubated sample relative to that of the native protein was evident from the changing shape of amide I band in the corresponding DUVRR spectra (Figure 4). As a result, the difference DUVRR spectrum between the solution phase of 4-day incubated lysozyme and the native protein (Figure 11D) did show a clear deviation from the difference spectrum between the spectra of α-helix and the spectrum of the disordered structures for homo-polypeptides. Both far-UV CD and DUVRR spectroscopy indicated the formation of ~10% β-sheet in the soluble fraction of the lysozyme sample incubated for 4 days. The discrepancy between the results of far-UV CD and DUVRR spectroscopic analysis can be attributed to the limited selectivity of CD spectroscopy to β-sheet and disordered structures [86].

The C_α–H bending bands in the difference DUVRR spectra (disordered structure vs. α-helix, Figure 11C) were utilized in quantifying α-helix melting. This is because: (i) the C_α–H bending band is isolated from the spectral contributions of other amide bands and the bands of aromatic side chains;

© 2008 by WILEY-VCH Verlag GmbH & Co. KGaA, Weinheim

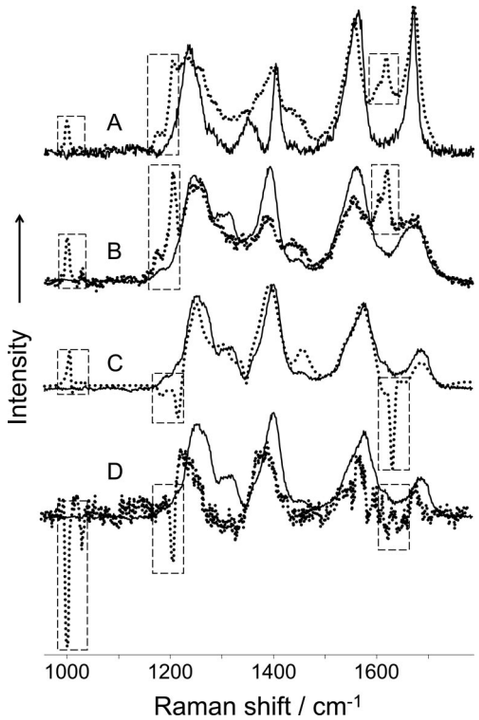

Figure 11 Comparison of DUVRR spectra of lysozyme and the basis DUVRR spectra (Sα, Sβ, Src represent the basis spectrum of α-helix, β-sheet and disordered structures, respectively) obtained from polypeptides PGA and PLL (see text for details). (A) basis spectrum of β-sheet (solid line, from PLL) and spectrum of lysozyme fibril (dotted line); (B) basis spectrum of disordered structures (solid, from PGA) and spectrum of the denatured-reduced lysozyme in HCl solution (dotted line); (C) fitted difference spectrum of denatured-reduced lysozyme in HCl and in 30% of TFE solution (dotted line) and the difference spectrum of the basis spectra (Src – Sα, solid line); (D) difference spectrum of the solution phase of 4-day-incubated lysozyme and the native lysozyme (dotted line) and the difference spectrum of the basis spectra (Src – Sα, solid line). The spectral contributions from phenylalanine and tyrosine side chains were circled with dashed rectangles.

(ii) it has a simple structure as compared with the complicated amide III band [67]. In addition, the α-helix makes no noticeable contribution to the DUVRR spectrum in the C_α–H bending region, while both β-sheet and disordered structures exhibit a strong C_α–H bending band [63, 79]. This means that even if there is a relatively small conversion between β-sheet and disordered structures, which may accompany the α-helix melting/formation, the major contribution to the change of C_α–H bending band will be determined by the change in α-helix content. Therefore, the percentages of the melted α-helix (Δ_α) for the incubated lysozyme can be calculated from the intensity of C_α–H bending bands (I_P) in the difference spectra.

$$\Delta_{\alpha,\,incb} = \frac{I_{P,\,incb}}{I_{P,\,d-r}} \cdot \Delta_{\alpha,\,d-r} \qquad (1)$$

The subscripts incb and d-r indicate the difference spectra of the incubated lysozyme (incubated minus native) and the denatured-reduced lysozyme (without TFE minus with 30% TFE), respectively.

Since far-UV CD spectroscopy determines α-helix accurately [86], the percentage of the α-helix formed due to the addition of 30% TFE to the denatured-reduced lysozyme ($\Delta_{\alpha,\,d-r}$) was set at 35% as determined by far-UV CD spectroscopy (Table 2, difference between the percentages of α-helix in 30% of TFE and pH 2.0 HCl solution). Using this approach, the α-helix melting of the 12-hour- and 8-day-incubated lysozyme were estimated to be 9% and 26%, respectively. Therefore, the native lysozyme containing 32% of α-helix [71] transformed into a 8% α-helix-containing partially unfolded intermediate before assembling into fibrils. The α-helix melting vs. incubation time is shown in Figure 12. The data fit well by a monoexponential function with a characteristic time of 25 ± 13 h. Although the uncertainty of the estimation was rather large, the characteristic time is in agreement with the kinetics of lysozyme unfolding discussed above. It is noteworthy that a brief heating of pH 2.0 lysozyme solution to 65 °C resulted in ~15% of α-helix melting, which is completely reversible (data not shown).

The quantitative approach described here, i.e. quantifying the lysozyme unfolding based on the intensity of the C_α–H bands, did not make full use of the structural information provided by DUVRR

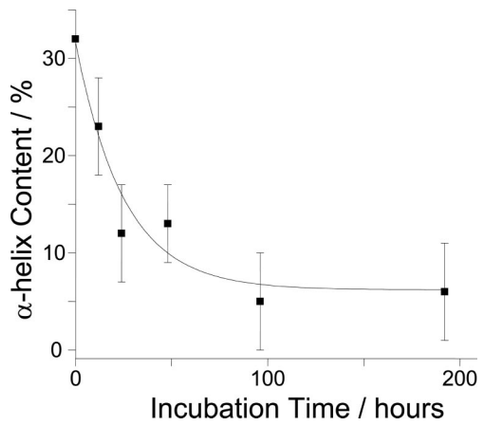

Figure 12 The α-helix melting of lysozyme resulted from prolonged incubation at 65 °C. The percentages of α-helix were calculated based on the DUVRR spectra of solution fractions of lysozyme incubated for various durations.

© 2008 by WILEY-VCH Verlag GmbH & Co. KGaA, Weinheim

Journal of
BIOPHOTONICS

spectroscopy. We plan to apply advanced statistical methods, chemometrics in particular [88, 89], to extract structural information from the spectroscopic data.

4.2 Kinetics of tertiary structural transition

Aromatic amino acid residues, tyrosine and tryptophan, are widely used as intrinsic fluorescent markers in protein folding studies [90–92]. The fluorescence [78], absorption [65, 78] and UV Raman [65] spectroscopic properties of tyrosine and tryptophan vary with the local environment either due to specific interaction with other amino acid residues or the changes of the exposure to water. Phenylalanine has not been used as a luminescent marker because of its very low quantum yield of fluorescence (~0.02) [78]. It has been, however, used as a Raman spectroscopic marker [93–96]. Spiro and coworkers [80] demonstrated that the 1000 cm^{-1} phenylalanine Raman band of ovomucoid third-domain proteins depends on its microenvironment. The authors have attributed their observation to the changes in phenylalanine local environment [80]. Hen egg white lysozyme is a monomeric globular protein. A cleft where the substrate binds divides the protein into two domains: α-domain and β-domain. Two of the three phenylalanine residues are located in the β-domain (Phe 3 and 38), and another one in the α-domain (Phe 34, in the α-helix). Four of the six tryptophan residues (Trp 28, 108, 111 and 123) are located in the α-domain, with the other two (Trp 62 and 63) in the β-domain facing the cleft. Because of the hydrophobic nature of the phenyl and indole group, the tryptophan and phenylalanine residue side chains are usually buried inside the hydrophobic environment. Therefore, the tertiary structural rearrangements of lysozyme can be studied by probing the changes of the microenvironment around both tryptophan and phenylalanine residues.

Figure 2 showed the evolution of lysozyme fluorescence spectra dominated by tryptophan emission as a function of the incubation time. The red shift of the fluorescence peak from 343 nm for the native lysozyme to 355 nm for the unfolded conformer (lysozyme incubated for more than 4 days) can be attributed to the changes in the local environment of tryptophan residues from nonpolar to polar. In other words, the tryptophan side chains of lysozyme became more exposed to water in the denatured conformation than it was in the native one. The kinetics of tryptophan fluorescence changes showed that the tertiary structural rearrangements occurred monoexponentially with a characteristic time of 32 ± 4 h.

When excitation wavelengths below 200 nm are used, strong resonance enhancement of Raman scattering occurs due to $B_{a,b}$ electronic transition of phenyl ring at ~188 nm [82]. The phenylalanine ν_{12} vibrational mode (1000 cm^{-1}) is very sensitive to the resonance enhancement: a 10 nm shift of the excitation wavelength from 194 nm to 204 nm diminishes the contribution of phenylalanine to the DUVRR spectrum of lysozyme [43]. *N*-acetyl-L-phenylalanine ethyl ester in acetonitrile-water cosolvent of different compositions was used to verify the dependence of the phenylalanine Raman signature on the local environment (Figure 6). The Raman cross section of the ν_{12} phenyl vibrational mode (1000 cm^{-1}) increased monotonically (up to threefold) with increasing acetonitrile content and reached saturation at ~50% of acetonitrile (Figure 6, inset). Although some solvent dependence was also evident for the ν_{18a} (1029 cm^{-1}) and ring-C (1205 cm^{-1}) modes, the ν_{12} band seemed to be the most useful marker band for probing the local environment of phenylalanine in protein because of two reasons: (i) ν_{12} is the most intense band at 197 nm excitation because of the resonance enhancement [81, 82]; (ii) the ν_{12} band is isolated from other Raman bands (tyrosine and amide bands) in the protein DUVRR spectra (Figure 4).

The intensity of the phenyl ν_{12} bands of the soluble phase of the incubated lysozyme decreased monoexponentially with a characteristic time of 29 ± 2 h (Figure 5). These changes can be attributed to the increased water exposure of phenylalanine side chains, as illustrated in Figure 6. The DUVRR data were in good agreement with the tryptophan fluorescence data and further confirms that the lysozyme tertiary structure changes monoexponentially with the incubation time.

The further decreased phenyl ν_{12} band in the DUVRR spectrum of lysozyme fibrils (Figure 4) indicated that phenylalanine side chains are strongly exposed to water in lysozyme fibrils. This could be an indication that phenylalanine residues are located in the unordered part of lysozyme fibrils. In contrast to the conventional tryptophan/tyrosine fluorescence, the phenylalanine DUVRR spectroscopic marker can be used for characterizing nonhomogeneous, light-scattering samples such as fibrils.

Interestingly, both secondary structure (according to DUVRR spectra of amide chromophore) and tertiary structure (according to tryptophan fluorescence and DUVRR signature of phenylalanine) of lysozyme evolved in a monoexponential fashion with characteristic time of about 30 h before the assembly into fibrils. This indicated that the partial unfolding of lysozyme is an all-or-none transition, i.e. two-state transition [88].

The DUVRR spectra of random-coil-rich and α-helix-rich lysozyme conformers showed distinctive differences in the amide II, amide III and C_α–H bending bands (Figure 10). Despite the higher α-he-

© 2008 by WILEY-VCH Verlag GmbH & Co. KGaA, Weinheim

lix content in the α-helix-rich conformer than in the native lysozyme (47% vs. 32%, Table 2), the phenylalanine ν_{12} vibrational mode (1000 cm^{-1}) did not change comparably with that found for the native lysozyme unfolding (such as in Figures 4B and C). This indicated that the protein did not form a well-defined tertiary structure in 30% TFE solution despite extensive α-helix formation. This observation is in agreement with the studies of Hoshino et al. [87] on the effect of TFE on lysozyme using CD spectroscopy and small-angle X-ray scattering (SAXS). According to their results, 11.1% of α-helix remained in the "disulfide bond-reduced and carboxymethylated" lysozyme, which is the equivalent of the "denatured-reduced lysozyme" in this study. The protein in TFE solution has been concluded to assume an open-helical structure with no or weak tertiary interactions [87].

5. Conclusion

The *in-vitro* hen egg white lysozyme fibril formation was studied by DUVRR spectroscopy, along with fluorescence and CD spectroscopy. The first step of the structural transition was found to be an irreversible unfolding, which resulted in a partially unfolded intermediate. The irreversible unfolding was characterized quantitatively by probing both the secondary and tertiary structural transitions with DUVRR, far-UV CD and fluorescence spectroscopy. Phenylalanine was shown to be a useful DUVRR biomarker for probing protein tertiary structural evolution.

Acknowledgement We thank Drs. Mikhail Savvateev and Pavel Dorozhkin (NT-MDT Co., Russia) for the technical support in the AFM measurements and the Research Corporation (RI1229, IKL) for financial support.

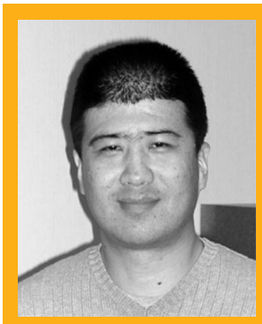

Mr. Ming Xu is a graduate student in Professor Igor Lednev's laboratory. He obtained an MS degree in Biochemistry and Molecular Biology from Shanghai Medical University (Shanghai, China) in 2001 and a Bachelor's degree in Nuclear Medicine from Suzhou Medical College (Suzhou, Jiangsu Province, China) in 1998.

Vladimir Ermolenkov is a Structural Chemistry Core Facility Director in the Life Sciences Research Building, University at Albany, SUNY. He obtained his PhD Degree in Optics and Laser Physics from Stepanov Institute of Physics, National Academy of Sciences of Belarus (Minsk, Belarus) in 2001. He was a Postdoctoral Associate in the research group of Professor Igor Lednev at the University at Albany during the period 2003–2006. He is the author of more than 80 publications in lasers and spectroscopy of complex and biological molecules.

Dr Uversky received broad training, with an MS in Physics (Leningrad State University, Russia, 1986), a PhD (Moscow Institute of Technical Physics, 1991) and a DSc in Biophysics (Institute of Experimental and Theoretical Biophysics, Russian Academy of Sciences, 1998) and with pre- and postdoctoral research in Structural Biology, Biochemistry and Biophysics (1991–1998, at the Institute of Protein Research, Russian Academy of Sciences). Since 1998 he worked for UCSC before taking his present appointment at IU in 2004. Dr Uversky is using various molecular biophysics methods to study protein folding, protein misfolding/aggregation and to characterize partially folded proteins. Working on protein folding-misfolding, Dr Uversky found that many biologically active proteins do not have rigid structure and are often involved in human diseases. While he continues to use biophysics, more recently Dr Uversky has focused on the development and use of bioinformatics methods for the study of intrinsically disordered proteins. Dr Uversky has authored over 250 scientific publications and edited several books and book series on protein structure, function, folding and misfolding. He is also an editor of several scientific journals.

Igor K. Lednev graduated from the Moscow Institute of Physics and Technology, Russian Federation, receiving his PhD degree in 1983. He then worked at the Institute of Chemical Physics, Russian Academy of Sciences as a group leader till 1994. Since *Perestroika*, Dr Lednev has been a visiting researcher at the University of York (with Prof. Ron Hester) and the

© 2008 by WILEY-VCH Verlag GmbH & Co. KGaA, Weinheim

University of Durham, UK (with Prof. Michael Petty). He also worked as an academic visitor in Japan and Canada, and as a research professor at the University of Pittsburgh, USA (with Prof. Sanford Asher). At present, Dr Lednev is an assistant professor at the University at Albany, State University of New York. His research is focused on the development and application of novel laser spectroscopy for biological and chemical studies. In particular, he recently built a new apparatus and developed a novel methodology, based on deep-ultraviolet Raman spectroscopy combined with advanced statistical analysis for structural characterization of proteins. Lednev's research group is also working on the application of advanced spectroscopy for forensic and environmental purposes. Dr Lednev is a current recipient of the Research Innovation Award. He has coauthored over 90 publications in peer-reviewed journals.

References

[1] C. M. Dobson, Nature **426**, 884 (2003).
[2] J. W. Kelly, Proc. Natl. Acad. Sci. USA **95**, 930 (1998).
[3] J. W. Kelly, Curr. Opin. Struct. Biol. **8**, 101 (1998).
[4] E. Bossy-Wetzel and R. Schwarzenbacher, S. A. Lipton, Nat. Med. **10**, S2 (2004).
[5] C. A. Ross and M. A. Poirier, Nat. Med. **10**, S10 (2004).
[6] L. A. Morozova-Roche, J. Zurdo, A. Spencer, W. Noppe, V. Receveur, D. B. Archer, M. Joniau, and C. M. Dobson, J. Struct. Biol. **130**, 339 (2000).
[7] M. B. Pepys, P. N. Hawkins, D. R. Booth, D. M. Vigushin, G. A. Tennent, A. K. Soutar, N. Totty, O. Nguyen, C. C. F. Blake, C. J. Terry, T. G. Feest, A. M. Zalin, and J. J. Hsuan, Nature **362**, 553 (1993).
[8] P. O. Souillac, V. N. Uversky, I. S. Millett, R. Khurana, S. Doniach, and A. L. Fink, J. Biol. Chem. **277**, 12657 (2002).
[9] R. S. Abraham, S. M. Geyer, M. Ramirez-Alvarado, T. L. Price-Troska, M. A. Gertz, and R. Fonseca, J. Clin. Immunol. **24**, 340 (2004).
[10] R. Wetzel, Adv. Protein Chem. **50**, 183 (1997).
[11] R. W. McLaughlin, J. K. De Stigter, L. A. Sikkink, E. M. Baden, and M. Ramirez-Alvarado, Protein Sci. **15**, 1710 (2006).
[12] S. Y. Tan and M. B. Pepys, Histopathology **25**, 403 (1994).
[13] V. Bellotti, P. Mangione, and M. Stoppini, Cell. Mol. Life Sci. **55**, 977 (1999).
[14] T. Ban, K. Yamaguchi, and Y. Goto, Acc. Chem. Res. **39**, 663 (2006).
[15] J. Goers, S. E. Permyakov, E. A. Permyakov, V. N. Uversky, and A.L. Fink, Biochemistry **41**, 12546 (2002).
[16] K. Takase, T. Higashi, and T. Omura, J. Protein Chem. **21**, 427 (2002).
[17] R. Khurana, C. Ionescu-Zanetti, M. Pope, J. Li, L. Nielson, M. Ramirez-Alvarado, L. Regan, A. L. Fink, and S. A. Carter, Biophys. J. **85**, 1135 (2003).
[18] A. Ahmad, I. S. Millett, S. Doniach, V. N. Uversky, and A. L. Fink, Biochemistry **42**, 11404 (2003).
[19] M. Fandrich, M. A. Fletcher, and C. M. Dobson, Nature **410**, 165 (2001).
[20] V. N. Uversky and A. L. Fink, Biochim. Biophys. Acta, **1698**, 131 (2004).
[21] I. K. Lednev, V. V. Ermolenkov, S. Higashiya, L. A. Popova, N. I. Topilina, and J. T. Welch, Biophys. J. **91**, 3805 (2006).
[22] N. I. Topilina, V. V. Ermolenkov, S. Higashiya, J. T. Welch, and I. K. Lednev, Biopolymers **86**, 261 (2007).
[23] N. I. Topilina, S. Higashiya, N. Rana, V. V. Ermolenkov, C. Kossow, A. Carlsen, S. C. Ngo, C. C. Wells, E. T. Eisenbraun, K. A. Dunn, I. K. Lednev, R. E. Geer, A. E. Kaloyeros, and J. T. Welch, Biomacromolecules **7**, 1104 (2006).
[24] J. D. Sipe and A. S. Cohen, J. Struct. Biol. **130**, 88 (2000).
[25] L. C. Serpell, Biochim. Biophys. Acta **1502**, 16 (2000).
[26] M. Sunde and C. C. F. Blake, Q. Rev. Biophys. **31**, 1 (1998).
[27] R. Tycko, Curr. Opin. Struct. Biol. **14**, 96 (2004).
[28] M. S. Forman, V. M. Y. Lee, and J. Q. Trojanowski, Trends Neurosci. **26**, 407 (2003).
[29] H. A. Lashuel, D. Hartley, B. M. Petre, T. Walz, and P. T. Lansbury, Jr. Nature **418**, 291 (2002).
[30] D. R. Booth, M. Sunde, V. Bellotti, C. V. Robinson, W. L. Hutchinson, P. E. Fraser, P. N. Hawkins, C. M. Dobson, S. E. Radford, C. C. F. Blake, and M. B. Pepys, Nature **385**, 787 (1997).
[31] D. Canet, A. M. Last, P. Tito, M. Sunde, A. Spencer, D. B. Archer, C. Redfield, C. V. Robinson, and C. M. Dobson, Nature Struct. Biol. **9**, 308 (2002).
[32] F. D. Sonnichsen, J. E. Van Eyk, R. S. Hodges, and B. D. Sykes, Biochemistry **31**, 8790 (1992).
[33] S. Goda, K. Takano, Y. Yamagata, R. Nagata, H. Akutsu, S. Maki, K. Namba, and K. Yutani, Protein Sci. **9**, 369 (2000).
[34] Y. Yonezawa, S. Tanaka, T. Kubota, K. Wakabayashi, K. Yutani, and S. Fujiwara, J. Mol. Biol. **323**, 237 (2002).
[35] Y. Fezoui and D. B. Teplow, J. Biol. Chem. **277**, 36948 (2002).
[36] A. Cao, D. Hu, and L. Lai, Protein Sci. **13**, 319 (2004).
[37] L. A. Munishkina, A. L. Fink, and V. N. Uversky, J. Mol. Biol. **342**, 1305 (2004).
[38] B. A. Vernaglia, J. Huang, and E. D. Clark, Biomacromolecules, **5**, 1362 (2004).
[39] T. N. Niraula, T. Konno, H. Li, H. Yamada, K. Akasaka, and H. Tachibana, Proc. Natl. Acad. Sci. USA **101**, 4089 (2004).
[40] M. R. H. Krebs, D. K. Wilkins, E. W. Chung, M. C. Pitkeathly, A. K. Chamberlain, J. Zurdo, C. V. Robinson, and C. M. Dobson, J. Mol. Biol. **300**, 541 (2000).
[41] E. Frare, P. Polverino de Laureto, J. Zurdo, C. M. Dobson, and A. Fontana, J. Mol. Biol. **340**, 1153 (2004).
[42] L. N. Arnaudov and R. De Vries, Biophys. J. **88**, 515 (2005).
[43] I. K. Lednev, V. V. Ermolenkov, W. He, and M. Xu, Anal. Bioanal. Chem. **381**, 431 (2005).

© 2008 by WILEY-VCH Verlag GmbH & Co. KGaA, Weinheim

[44] A. K. Chamberlain, V. Receveur, A. Spencer, C. Redfield, and C. M. Dobson, Protein Sci. **10**, 2525 (2001).
[45] M. Dumoulin, D. Canet, A. M. Last, E. Pardon, D. B. Archer, S. Muyldermans, L. Wyns, A. Matagne, C. V. Robinson, C. Redfield, and C. M. Dobson, J. Mol. Biol. **346**, 773 (2005).
[46] M. Ramirez-Alvarado, M. J. Cocco, and L. Regan, Protein Sci. **12**, 567 (2003).
[47] R. Khurana, J. R. Gillespie, A. Talapatra, L. J. Minert, C. Ionescu-Zanetti, I. Millett, and A. L. Fink, Biochemistry **40**, 3525 (2001).
[48] K. Lu, J. Jacob, P. Thiyagarajan, V. P. Conticello, and D. G. Lynn, J. Am. Chem. Soc. **125**, 6391 (2003).
[49] M. Tanaka, Y. Machida, Y. Nishikawa, T. Akagi, T. Hashikawa, T. Fujisawa, and N. Nukina, J. Biol. Chem. **278**, 34717 (2003).
[50] T. Ban, M. Hoshino, S. Takahashi, D. Hamada, K. Hasegawa, H. Naiki, and Y. Goto, J. Mol. Biol. **344**, 757 (2004).
[51] W. Liu, J. M. Prausnitz, and H. W. Blanch, Biomacromolecules **5**, 1818 (2004).
[52] M. R. Nilsson and C. M. Dobson, Biochemistry **42**, 375 (2003).
[53] H. Azakami, A. Mukai, and A. Kato, J. Agric. Food Chem. **53**, 1254 (2005).
[54] J. Li, V. N. Uversky, and A. L. Fink, Neurotoxicology **23**, 553 (2002).
[55] C. L. Shen and R. M. Murphy, Biophys. J. **69**, 640 (1995).
[56] M. M. Pallitto and R. M. Murphy, Biophys. J. **81**, 1805 (2001).
[57] Z. Gu, X. Zhu, S. Ni, Z. Su, and H.-M. Zhou, Int. J. Biochem. Cell Biol. **36**, 795 (2004).
[58] A. L. Fink, Acc. Chem. Res. 39, 628 (2006).
[59] M. Xu, V. V. Ermolenkov, W. He, V. N. Uversky, L. Fredriksen, and I. K. Lednev, Biopolymers **79**, 58 (2005).
[60] S. A. Asher, in Handbook of Vibrational Spectroscopy, Vol. 1, (John Wiley & Sons Ltd., 2001) pp. 557.
[61] V. Shashilov, M. Xu, V. V. Ermolenkov, L. Fredriksen, and I. K. Lednev, J. Am. Chem. Soc. **129**, 6972 (2007).
[62] M. Xu, V. Shashilov, and I. K. Lednev, J. Am. Chem. Soc. **129**, 11002 (2007).
[63] Z. Chi, X. G. Chen, J. S. Holtz, and S. A. Asher, Biochemistry **37**, 2854 (1998).
[64] C.-Y. Huang, G. Balakrishnan, and T. G. Spiro, J. Raman Spectrosc. **37**, 277 (2006).
[65] Z. Chi and S. A. Asher, J. Phys. Chem. B **102**, 9595 (1998).
[66] I. K. Lednev, in Methods in Protein Structures and Stability Analysis: Part B. Vibrational Spectroscopy, eds. V. N. Uversky and E. A. Permyakov, in Molecular Anatomy and Proteins, series ed. V. N. Uversky (Nova Science Publishers, Inc., New York, 2007).
[67] A. V. Mikhonin, Z. Ahmed, A. Ianoul, and S. A. Asher, J. Phys. Chem. B **108**, 19020 (2004).
[68] C. C. F. Blake, R. H. Fenn, A. C. T. North, D. C. Phillips, and R. J. Poljak, Nature **196**, 1173 (1962).
[69] C. M. Dobson, P. A. Evans, and S. E. Radford, Trends Biochem. Sci. **19**, 31 (1994).
[70] C. Redfield and C. M. Dobson, Biochemistry **27**, 122 (1988).
[71] M. Ramin, W. Shepard, R. Fourme, and R. Kahn, Acta Crystallogr. D Biol. Crystallogr. **55**, 157 (1999).
[72] V. P. Saxena and D. B. Wetlaufer, Biochemistry **9**, 5015 (1970).
[73] N. Sreerama and R. W. Woody, Anal. Biochem. **287**, 252 (2000).
[74] N. Sreerama and R. W. Woody, Anal. Biochem. **209**, 32 (1993).
[75] W. C. Johnson, Proteins: Struct. Func. Genet. **35**, 307 (1999).
[76] S. W. Provencher and J. Glockner, Biochemistry **20**, 33 (1981).
[77] A. K. Chamberlain, C. E. MacPhee, J. Zurdo, L. A. Morozova-Roche, H. A. O. Hill, C. M. Dobson, and J. J. Davis, Biophys. J. **79**, 3282 (2000).
[78] A. P. Demchenko, Ultraviolet Spectroscopy of Proteins, (Springer-Verlag, Berlin, 1986).
[79] Y. Wang, R. Purrello, T. Jordan, and T. G. Spiro, J. Am. Chem. Soc. **113**, 6359 (1991).
[80] P. G. Hildebrandt, R. A. Copeland, T. G. Spiro, J. Otlewski, M. Laskowski, Jr. and F. G. Prendergast, Biochemistry, **27**, 5426 (1988).
[81] S. A. Asher, M. Ludwig, and C. R. Johnson, J. Am. Chem. Soc. **108**, 3186 (1986).
[82] S. P. A. Fodor, R. A. Copeland, C. A. Grygon, and T. G. Spiro, J. Am. Chem. Soc. **111**, 5509 (1989).
[83] M. Ramirez-Alvarado and L. Regan, J. Mol. Biol. **323**, 17 (2002).
[84] K. R. Babu and V. Bhakuni, Eur. J. Biochem. **245**, 781 (1997).
[85] I. K. Lednev, A. S. Karnoup, M. C. Sparrow, and S. A. Asher, J. Am. Chem. Soc. **121**, 8074 (1999).
[86] A. Rodger and B. Norden, Circular Dichroism and Linear Dichroism, (Oxford University Press, Oxford, UK, 1997).
[87] M. Hoshino, Y. Hagihara, D. Hamada, M. Kataoka, and Y. Goto, FEBS Lett. **416**, 72 (1997).
[88] M. Xu, V. A. Shashilov, V. V. Ermolenkov, L. Fredriksen, D. Zagorevski, and I. K. Lednev, Protein Sci. **16**, 815 (2007).
[89] V. A. Shashilov, M. Xu, V. V. Ermolenkov, and I. K. Lednev, J. Quantum. Spectrosc. Radiat. Transf. **102**, 46 (2006).
[90] W. Y. Yang and M. Gruebele, J. Am. Chem. Soc. **126**, 7758 (2004).
[91] V. Munoz, P. A. Thompson, J. Hofrichter, and W. A. Eaton, Nature **390**, 196 (1997).
[92] P. A. Thompson, V. Munoz, G. S. Jas, E. R. Henry, W. A. Eaton, and J. Hofrichter, J. Phys. Chem. B **104**, 378 (2000).
[93] N.-T. Yu and E. J. East, J. Biol. Chem. **250**, 2196 (1975).
[94] P. R. Carey, P. Fast, H. Kaplan, and M. Pozsgay, Biochim. Biophys. Acta **872**, 169 (1986).
[95] C. A. Grygon, J. R. Perno, S. P. A. Fodor, and T. G. Spiro, BioTechniques **6**, 50 (1988).
[96] J. B. Kneipp, Gurusamy, and T. G. Spiro, J. Phys. Chem. B **108**, 15919 (2004).

© 2008 by WILEY-VCH Verlag GmbH & Co. KGaA, Weinheim